

# 1 A Taylor's power law in the Wenchuan earthquake sequence with 2 fluctuation scaling

3  
4 Peijian Shi<sup>1</sup>, Mei Li<sup>2\*</sup>, Yang Li<sup>3\*</sup>, Jie Liu<sup>2</sup>, Haixia Shi<sup>2</sup>, Tao Xie<sup>2</sup>, Chong Yue<sup>2</sup>

5  
6 <sup>1</sup>Co-Innovation Center for Sustainable Forestry in Southern China, College of Biology and the  
7 Environment, Bamboo Research Institute, Nanjing Forestry University, Nanjing 210037, China

8 <sup>2</sup>China Earthquake Networks Center, China Earthquake Administration, Beijing 100045, China

9 <sup>3</sup>Department of Mathematics and Statistics, University of Minnesota Duluth, Duluth, MN 55812, USA

10 *Correspondence to:* mei\_seis@163.com (M. Li); yangli@d.umn.edu (Y. Li)

11  
12 **Abstract** Taylor's power law (TPL) describes the scaling relationship between the  
13 temporal or spatial variance and mean of population densities by a simple power law.

14 TPL has been widely testified across space and time in biomedical sciences, botany,  
15 ecology, economics, epidemiology, and other fields. In this paper, TPL is analytically

16 reconfirmed by testifying the variance as a function of the mean of the released  
17 energy of earthquakes with different magnitudes on varying timescales during the

18 Wenchuan earthquake sequence. Estimates of the exponent of TPL are approximately  
19 2, showing that there is mutual attraction among the events in the sequence. **On the**

20 **other hand, the spatial–temporal distribution of the Wenchuan aftershocks tends to be**  
21 **nonrandom, whereas the scaling relationship between the variance and mean of the**

22 **energy release from aftershocks is approximately definite and deterministic.** Effect of  
23 different divisions on estimation of the intercept of TPL straight line has been

24 checked while the exponent is kept to be 2. The result shows that the intercept acts as  
25 a logarithm function of the time division. It implies that the mean–variance

26 relationship of the energy release from the earthquakes can be quantified although we  
27 cannot accurately predict the occurrence time and locations of imminent events.

28

## 29 **0 Introduction**

30 The Wenchuan  $M_S$  8.0 earthquake on May 12, 2008 was the result of the  
31 intensively compressive movement between the Qinghai–Tibet Plateau and the  
32 Sichuan basin. It ruptured the middle segment of the Longmenshan (LMS) thrust belt  
33 (Burchfiel et al., 2008), with a total length of fault trace of approximately 400 km  
34 along the edge of the Sichuan basin and the eastern margin of the Tibetan plateau, in  
35 the middle of the north–south seismic belt of China. Millions of aftershocks have  
36 occurred after the main event. Up to now, the focus zone tends to be quiet with only  
37 small ones occurring occasionally. A complete Wenchuan earthquake sequence has  
38 been attained.

39 Statistical seismology applies statistical methods to the investigation of seismic  
40 activities, and stochastic point process theory promotes the development of statistical  
41 seismology (Vere–Jones et al., 2005). After some improvement, most of the  
42 point process theories and methods can be used to analyze spatio–temporal data of  
43 earthquake occurrence and to describe active laws of aftershocks. The term  
44 “aftershock” is widely used to refer to those earthquakes which follow the occurrence  
45 of a large earthquake and aggregately take place in abundance within a limited  
46 interval of space and time. This population of earthquakes is usually called an  
47 earthquake sequence. In seismological investigations, one important subjects has long  
48 been to the statistical properties of the aftershocks. Spatial and temporal distribution

49 of aftershocks after a destructive earthquake is usually performed in a general survey  
50 (Utsu, 1969). In seismology, one of the most famous theories describing the activities  
51 of aftershocks is the Gutenberg–Richter law (Gutenberg and Richter, 1956), which  
52 expresses the relationship between the magnitude and the total number of earthquakes  
53 with at least that magnitude in any given region and time interval. Another one is the  
54 Omori's law, which was first depicted by Fusakichi Omori in 1894 (Omori, 1894) and  
55 shows that the frequency of aftershocks decreases roughly with the reciprocal of time  
56 after the main shock. Utsu et al. (1969, 2009) developed this law and proposed the  
57 modified Omori formula afterwards. Since the 1980s, with the development of  
58 nonlinear theory, an epidemic–type aftershock sequence (ETAS) model has been  
59 proposed by Ogata (1988, 1989, 1999), which is based on the empirical laws of  
60 aftershocks and quantifies the dynamic forecasting of the induced effects. This model  
61 has been used broadly in earthquake sequence study (Kumazawa and Ogata, 2013;  
62 Console, 2010).

63 An increasing number of investigations show that there is an interaction effect for  
64 the occurrence of aftershocks in a given area. Stress triggering model is usually used  
65 to depict interaction between larger earthquakes by the view of physics (Haris, 1998;  
66 Stein, 1999). More and more results show that obvious enhancement in Coulomb  
67 stress not only promotes the occurrence of upcoming mid or strong events of an  
68 earthquake sequence but also affects their spatial distribution to some degree  
69 (Robinson and Zhou, 2005).

70 The goal of this paper is to introduce a different statistical method called Taylor's

71 power law into the statistical seismology field by analyzing the Wenchuan earthquake  
72 sequence from the point of view of energy distribution or energy release. We aim to  
73 find out whether or not the energy distribution or energy release of the Wenchuan  
74 earthquake sequence complies with a specific power-law function of TPL for  
75 different scaled samples, and what the spatial and temporal properties are.

76 In statistics, there are two important moments in a distribution, the mean ( $\mu$ )  
77 and the variance ( $\sigma^2$ ). It is common to describe the types of the distributions using the  
78 relationship between these two parameters. For instance, we have  $\sigma^2 = \mu$  for a Poisson  
79 distribution. In nature, however, the variance is not always equal to or proportional to  
80 the mean. Mutual attraction or mutual repulsion for individuals in natural populations,  
81 e.g., the intra-specific completion of plants, makes variance different from the mean.  
82 After examining many sets of samples of animal and plant population spatial densities,  
83 Taylor (1961) found that the variance appears to be related to the mean by a power-  
84 law function: the variance is proportional to the mean raised to a certain power

$$85 \quad \sigma^2 = a\mu^b \quad (1)$$

86 or equivalently as a linear function when the mean and variance are both  
87 logarithmically transformed

$$88 \quad \log_{10}(\sigma^2) = \log_{10}(a) + b \times \log_{10}(\mu) = c + b \times \log_{10}(\mu) \quad (2)$$

89 where  $a$  and  $b$  are constants and  $c = \log_{10}(a)$ . Eqs. 1 or 2 is called Taylor's power law  
90 (henceforth TPL) or Taylor's power law of fluctuation scaling (Eisler et al., 2008).

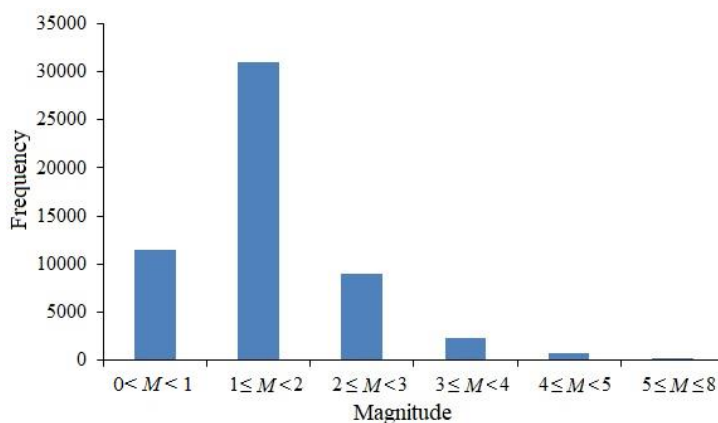
91 Eqs. 1 and 2 may be exact if the mean and variance are population moments  
92 calculated from certain parametric families of skewed probability distributions

93 (Cohen and Xu, 2015). TPL describes the species-specific relationship between the  
94 spatial or temporal variance of populations and their mean abundances (Kilpatrick and  
95 Ives, 2003). It has been verified for hundreds of biological species and nonbiological  
96 quantities in biomedical sciences, botany, ecology, epidemiology, biomedical sciences,  
97 botany, and other fields (Taylor, 1961, 1984; Kendal, 2002; Eisler et al., 2008; Cohen  
98 and Xu, 2015; Shi et al., 2016, 2017; Lin et al., 2018). Most of the scientific  
99 investigations of TPL mainly focus on the power-law exponent  $b$  (or slope  $b$  in the  
100 linear form), which has been believed to contain information on aggregation in space  
101 or time of populations for a certain species (Horne and Schneider, 1995).

102 In this study, we also concentrate on the parameter  $b$  of TPL. We expect that  $b$  is  
103 independent of the temporal block size  $A$  which is used to divide the Wenchuan  
104 sequence into different temporal blocks because the aftershock area is invariable  
105 during this period.

## 106 **1 Wenchuan earthquake sequence**

107



108

109 Figure 1 Histogram of earthquakes with different magnitudes of the Wenchuan sequence.

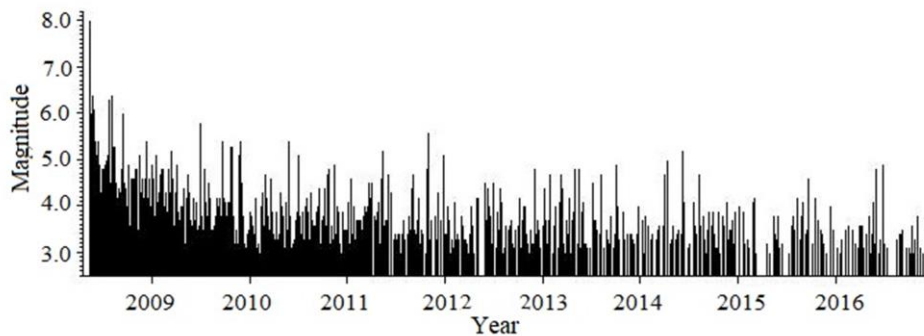
110

111 A large earthquake of magnitude  $M_S$  8.0 hit Wenchuan, Sichuan province of  
112 China at 14:28:01 CST (China Standard Time) on May 12, 2008 with an epicenter  
113 located at 103.4  $^{\circ}$ N and 31.0  $^{\circ}$ E and a depth of 19 km.

114 According to the earthquake catalogue of the China Earthquake Networks Center  
115 (CENC) (<http://www.csi.ac.cn/>), there have been 54,554 earthquakes of magnitudes  
116  $M > 0$  recorded for the Wenchuan sequence by December 31, 2016. Figure 1 shows  
117 the frequency of aftershocks with different magnitudes. Here, aftershocks with  $M <$   
118 2.0 account for 77.9% of the total sequence due to the fact that only weak ones occur  
119 after a long period of time after the main shock. In addition, except for the main shock,  
120 the number of aftershocks is 733 for magnitudes  $4.0 \leq M < 5.0$ , and 86 for  $5.0 \leq M <$   
121 8.0, respectively. They account for a very small percentage of the total.

122

123



127

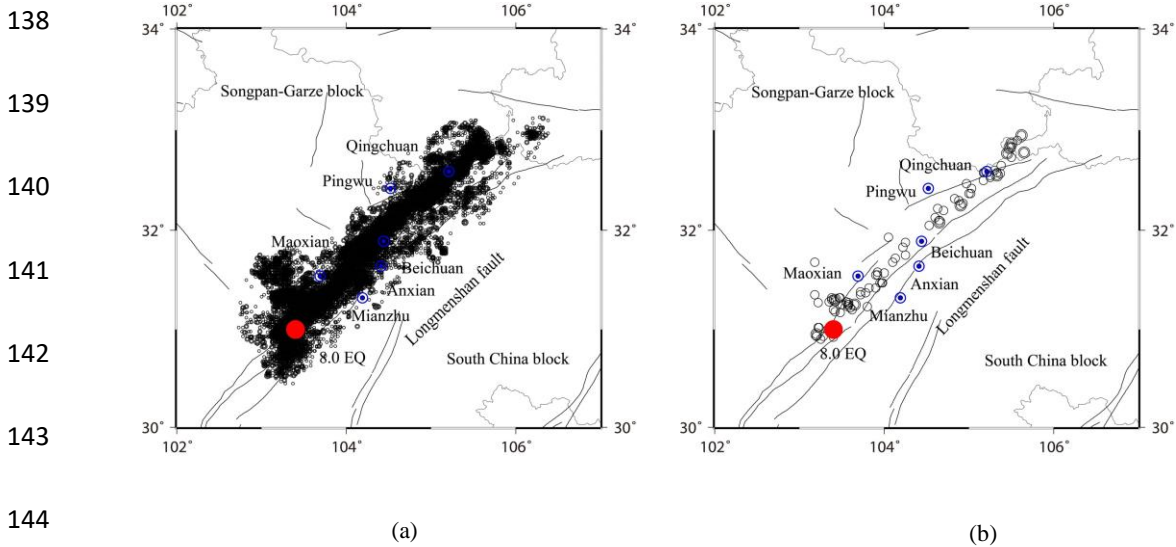
128 Figure 2 Series plot of the Wenchuan earthquake sequence with  $M \geq 3.0$  from May 12, 2008 to  
129 December 31, 2016.

130

131 Figure 2 displays the fluctuation variability of the Wenchuan earthquake  
132 sequence with  $M \geq 3.0$  from May 12, 2008 to December 31, 2016. The temporal  
133 distribution of the magnitudes of aftershocks attenuates quickly after the main shock.

134 The three larger aftershocks all occurred in 2008 with  $M$  6.4 on May 25,  $M$  6.1 on  
 135 August 1, and  $M$  6.1 on August 5, respectively. Eighty-five percent of aftershocks  
 136 with  $M \geq 3.0$  occurred by the end of 2011, about 2.5 years after the main shock.

137



145 Figure 3 Spatial distribution of epicenters of the Wenchuan earthquake sequences with (a)  $M > 0$  and (b)  
 146  $M \geq 5.0$  from May 12, 2008 to December 31, 2016. The main shock on May 12, 2008 is labeled by a  
 147 red solid circle.

148

149 Figure 3a shows the spatial distribution of epicenters of the Wenchuan  
 150 earthquake sequence with  $M > 0$  from May 12, 2008 to December 31, 2016. The  
 151 aftershocks are distributed in the region with latitude  $102^{\circ}\text{E}$ – $107^{\circ}\text{E}$  and longitude  
 152  $30^{\circ}\text{N}$ – $34^{\circ}\text{N}$ , mainly along the Longmenshan thrust fault, which is a junction region of  
 153 Songpan–Garze block and South China block and extends along north–east–east  
 154 (NEE) direction for more than 400 km. The size of the aftershocks on different scales  
 155 is characterized by a population density of the events distributed in space and time  
 156 after the Wenchuan  $M_S$  8.0 earthquake but we neglect the variations of the aftershock  
 157 area in the next step. The distribution of strong aftershocks is of different segment

158 characteristics. Earthquakes with magnitude  $M \geq 5.0$  mainly spread in south Miaoxian  
159 and Mianzhu area and north Pingwu area. There are no strong aftershocks occurring  
160 in the middle areas such as Beichuan and Anxian (see Figure 3b). According to the  
161 primary investigation results of the Wenchuan rupture process conducted by Chen et  
162 al. (2008), the rupture of the Wenchuan 8.0 earthquake originated from Wenchuan  
163 thrust fault with a little right lateral slip component and extended mainly in north–east  
164 (NE) orientation. The whole process formed two areas with larger dislocations. One is  
165 the south area of Miaoxian located in the bottom section in Figure 3b. The other one  
166 lies near Beichuan area (the middle segment in Figure 3b) but no strong shocks  
167 happened there.

168

## 169 **2 Data processing method**

170 For the complete Wenchuan earthquake sequence, we denote the number of all  
171 earthquakes by  $N$ , i.e.,  $N = 54,554$ , and use  $q = 1, \dots, N$  to index each earthquake. For  
172 each earthquake with magnitude  $M_q$ , its corresponding energy release is labeled by  $E_q$   
173 and it can be attained in the light of the following relationship (Xu and Zhou, 1982)

$$174 \quad \log_{10}(E_q) = 11.8 + 1.5M_q \quad (3)$$

175 We use  $t_q$  to index the time lag of the  $q$ -th aftershock from the main shock (in  
176 days), i.e.,  $t_1 = 0$  for the main event. The last aftershock occurred at 18:05:57 CST  
177 (China Standard Time) on December 31, 2016, and its  $t_q$  value is 3155.

178 In order to study the relationship between the variance and mean of the energy  
179 sequence  $E_q$ , we first divide it into equally–spaced short temporal blocks with size  $A$



180 (in days). For example, if  $A = 10$ , then the number of blocks is  $N/A = 3155/10 = 315.5$   
 181 which is rounded to the nearest integer. Now the complete energy sequence  $E_q$  is  
 182 partitioned into  $n = 316$  blocks of short energy subsequences. We use  $i$  to index each  
 183 block, i.e.,  $i = 1, \dots, n$  and  $h_i$  to denote the number of data points in each block which  
 184 is variable because earthquakes occurred stochastically in the sequence. Now we can  
 185 calculate the mean ( $\mu$ ) and variance ( $\sigma^2$ ) for each block using

$$186 \quad \mu_i = \frac{\sum_{j=1}^{h_i} E_{i,j}}{h_i} \quad (4)$$

$$187 \quad \sigma_i^2 = \frac{\sum_{j=1}^{h_i} (E_{i,j} - \mu_i)^2}{h_i - 1} \quad (5)$$

188 where  $E_{i,j}$  denotes the energy of the  $j$ -th earthquake in the  $i$ -th block.

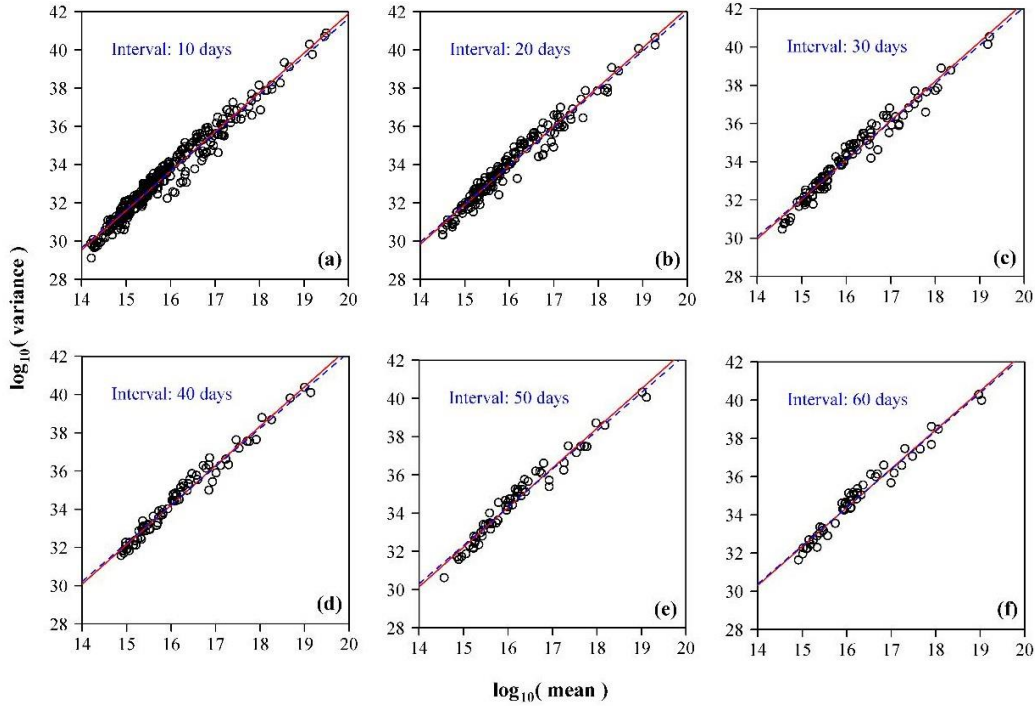
189

### 190 **3 Results**

191 The data processing procedure has been performed with different block size  $A =$   
 192 4, 5, 6, ..., 100. The number of sample points in each block decreases as the block  
 193 size increases. The relationships between the mean and variance of the released  
 194 energies from earthquakes in 6 representative temporal blocks are shown in Figure 4  
 195 on a log-log scale. The red line stands for the fitted linear function of TPL's power  
 196 law  $\log_{10}(\sigma^2) = c + b \log_{10}(\mu)$  using least squares. The 95% confidence intervals (CI)  
 197 of the slope and the coefficients of determination  $R^2$  are shown in Table S1. For  
 198 instance, Figure 4a shows the variance as a function of the mean for 316 time  
 199 intervals when  $A = 10$ . The estimated intercept is 0.702 and the estimated slope is  
 200 2.060 with a 95% CI of (1.989, 2.076) and  $R^2 = 0.963$ . The root-mean-square error  
 201 (RMSE) was also calculated to exhibit the feasibility of using a TPL with the

202 exponent 2 to approximate that with the exponent to be estimated (unknown).

203



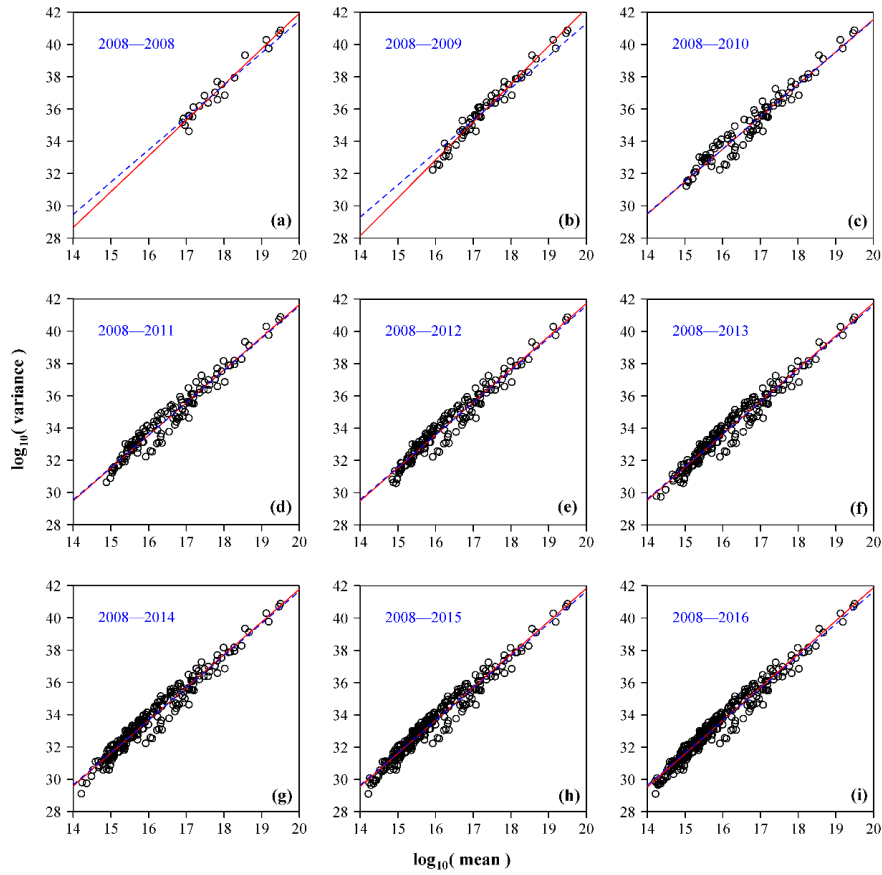
204

205 Figure 4 The calculated variance as a function of the observed mean of the energies from  
206 earthquakes in each time interval on log–log coordinates (open circles), for different values of  $A$ . The  
207 red straight line corresponds to the fitted Taylor's power law with an unknown exponent, i.e.  $\log_{10}(\sigma^2) =$   
208  $c + b \log_{10}(\mu)$ , using least squares. The blue dashed line corresponds to the fitted Taylor's power law  
209 with the exponent 2, i.e.  $\log_{10}(\sigma^2) = d + 2 \log_{10}(\mu)$ . There are 14 different values of  $A$  in total, and only  
210 6 are shown here. (a)  $A = 10$ ; (b)  $A = 20$ ; (c)  $A = 30$ ; (d)  $A = 40$ ; (e)  $A = 50$ ; and (f)  $A = 60$ .

211

212 Figure 4 and Table S1 show that there is an apparent linear relationship between  
213 the common logarithm of the variance and the common logarithm of the mean for all  
214 earthquakes occurring within different temporal blocks, characterized by a property of  
215 aggregation at different timescales. The estimated value of the intercept,  $c$  (or  
216  $\log_{10}(a)$ ), which is mainly influenced by the number of samples, overall increases with  
217  $A$  from 0.016 to 3.249 (Table S1). The estimates of slope  $b$ , on the other hand, are

218 roughly 2 for all block sizes used in the study. All  $R^2$  values are greater than 0.96,  
 219 showing a very strong linear relationship. These results indicate that the energy  
 220 release of aftershocks of the Wenchuan sequence complies well with a temporal TPL.



221  
 222 Figure 5 The calculated variance as a function of the observed mean of the energies from earthquakes  
 223 in each block on a log–log scale (open circles) when  $A$  is fixed to be 10. The red straight line  
 224 corresponds to the fitted Taylor's power law with an unknown exponent, i.e.  $\log_{10}(\sigma^2) = c + b \log_{10}(\mu)$ ,  
 225 using least squares. The blue dashed line corresponds to the fitted Taylor's power law with the  
 226 exponent 2, i.e.  $\log_{10}(\sigma^2) = d + 2 \log_{10}(\mu)$ . (a) 2008–2008; (b) 2008–2009; (c) 2008–2010; (d) 2008–  
 227 2011; (e) 2008–2012; (f) 2008–2013; (g) 2008–2014; (h) 2008–2015; and (i) 2008–2016.

228

229 Next, we divide the Wenchuan earthquake sequence into 9 time stages in years:  
 230 2008–2008, 2008–2009, 2008–2010, 2008–2011, 2008–2012, 2008–2013, 2008–2014,  
 231 2008–2015, and 2008–2016. For each stage, we follow a similar procedure leading to

232 Figure 4. That is, we first transform all earthquakes into their energy forms using the  
233 relationship between earthquake magnitude  $M$  and energy  $E$ . Then the energy  
234 sequence are partitioned into temporal blocks with a fixed block size  $A = 10$  days. The  
235 calculated variances and means are plotted on a log-log scale as shown in Figure 5.  
236 Again, TPL comes into play for all time stages. The estimates of the parameters in Eq.  
237 (2) for the data in different stages were listed in Table S2.

238 Figure 5 shows a strong linear relationship between the variance and mean of  
239 the earthquake energy populations on a log-log scale, especially for those large  
240 samples. The estimates summarized in Table S2 (red fitted lines in Figure 5) show  
241 similar results as in Table S1. The intercept gradually increases as the total number of  
242 samples increases but with a little more fluctuation. Meanwhile, the estimate of slope  
243  $b$  is still roughly a constant around 2.

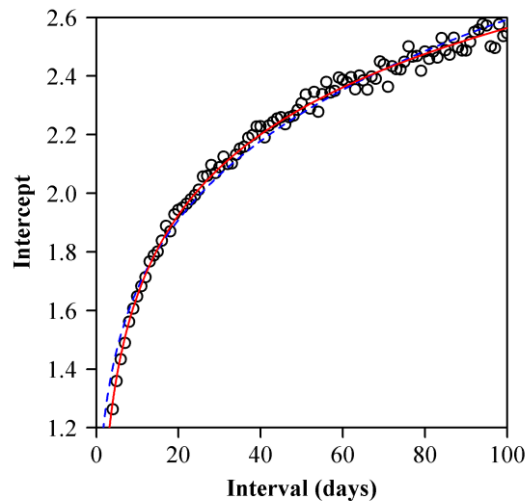
244 Because the variance of released energy from aftershocks in different temporal  
245 blocks is demonstrated to be proportional to the mean squared, we also examine the  
246 possible relationship between the estimate of the intercept (namely  $d$ ) in equation  
247  $\log_{10}(\sigma^2) = d + 2 \log_{10}(\mu)$  and the temporal block size  $A$ . The estimated intercepts of  
248 the Wenchuan sequence as  $A$  increases from 4 days to 100 days with 1 day increment  
249 are shown in Figure 6. We use a logarithm function and an exponential function to fit  
250 the data (i.e.,  $d = \alpha + \beta \times \log_{10}(A)$  and  $d = m \times A^n$ , where  $\alpha$ ,  $\beta$ ,  $m$  and  $n$  are constants),  
251 and find that the logarithm function has a better goodness of fit (namely a lower  
252 residual sum of squares). The estimate of parameter  $\alpha$  is equal to 0.7398 with 95% CI  
253 (0.7246, 0.7581), and the estimate of parameter  $\beta$  is equal to 0.9121 with 95% CI

254 (0.9004, 0.9229). Because  $\log_{10}(a) = d = \alpha + \beta \times \log_{10}(A)$ , we will have:

$$255 \quad \sigma^2 = a\mu^2 = 10^\alpha A^\beta \mu^2 \quad (6)$$

256 It illustrates that the variance of energy releases from aftershocks depends on two  
257 factors: (i) the mean squared, and (ii) the size of temporal block we define. Up to  
258 now, we confirm that the mean–variance relationship of energy releases from an  
259 earthquake sequence can be quantified although the accurate prediction of the time  
260 and location of an imminent event is still not attainable.

261



262

263 Figure 6 The effect of time division (time span) on the estimate of the intercept in the TPL with a fixed  
264 exponent of 2, i.e.  $\log_{10}(\sigma^2) = d + 2 \log_{10}(\mu)$ , where  $d$  denotes the intercept. Two equations were used to  
265 fit the data ( $d = \alpha + \beta \times \log_{10}(A)$  and  $d = m \times A^n$ , where  $\alpha, \beta, m$  and  $n$  are constants). The residual sum  
266 of squares (= 0.0535) using the logarithm function (represented by the red curve) is lower than that (=  
267 0.1460) using the exponential function (represented by the blue curve).

268

#### 269 **4 Discussion and conclusions**

270 The evolutionary process of a large earthquake is characterized by some complex  
271 features from stochastic to chaotic or pseudo–periodic dynamics (McCaffrey, 2011).

272 On the one hand, there is a long-term slow strain of accumulation and culminating of  
273 rocks in the rigid lithosphere prior to the event with a sudden rupture and  
274 displacement of blocks. On the other hand, there is another long-term slow strain of  
275 redistribution and energy release with a large number of aftershock occurrences in an  
276 extensive area, which generally lasts for several months, sometimes even years, after  
277 the main shock.

278 It has been statistically established that in populations, if individuals distribute  
279 randomly and are independent of each other, then the variance is equal to the mean,  
280 i.e.,  $\sigma^2 = \mu$ ; individuals show mutual attraction if the variance is proportional to the  
281 mean to a power  $> 1$ , i.e.,  $\sigma^2 > \mu$ ; individuals mutually repel each other if the  
282 variance is proportional to the mean to a power  $< 1$ , i.e.,  $\sigma^2 < \mu$  (Taylor, 1961; Horne  
283 and Schneider, 1995). The results obtained in this study show that the exponent of the  
284 TPL is around 2 in the Wenchuan energy sequence either with different time span  $A =$   
285 4, 5, 6, ..., 100 days or with a fixed time span  $A = 10$  days but for 9 time stages  
286 between 2008 and 2016. This means earthquakes in the Wenchuan sequence are not  
287 distributed at random and independent of each other but with a mutual attraction. It  
288 also indicates that there are possible interactions among different magnitudes in the  
289 earthquake sequence. Cohen and Xu (2015) proposed analytically that observations  
290 randomly sampled in blocks from any skewed frequency distribution with four finite  
291 moments give rise to TPL because the variation in the sample mean and sample  
292 variance between blocks are theoretically small if every block is randomly sampled  
293 from the same distribution.

294 There are various types of interpretations for the value of parameter  $b$ . Ford and  
295 Andrew (2007) suggested that individuals' reproductive correlation determines the  
296 size of  $b$ . While Kilpatrick and Ives (2003) proposed that interspecific competition  
297 could reduce the value of  $b$ . Above all, empirically,  $b$  usually lies between 1 and 2  
298 (Maurer and Taper, 2002). However, it is expected that TPL holds with  $b = 2$  exactly  
299 in a population with a constant coefficient of variation (CV) of population density.  
300 This expectation derives from the well-known relationship: SD (standard deviation)  
301 equals to square root of variance ( $\sigma^2$ ), i.e.,  $SD = \sigma$  and the coefficient of variation  
302  $CV = SD/\mu = k$ , here  $k$  is a constant. Then we can obtain  $\sigma^2 = (k\mu)^2$ . The relationship  
303 between  $\log_{10}(\sigma^2)$  and  $\log_{10}(k\mu)$  is a straight line with slope 2 on a log-log scale.

304 It is well established that there is a specific property on the population either in  
305 space or in time when  $b$  equals 2. Ballantyne (2005) proposed that  $b = 2$  is a  
306 consequence of deterministic population growth. While Cohen (2013) showed that  $b =$   
307 2 arose from exponentially growing, noninteracting clones. Furthermore, using the  
308 Lewontin-Cohen (LC) model of stochastic population dynamics, Cohen et al. (2015)  
309 provided an explicit, exact interpretation of its parameters of TPL. They proposed that  
310 the exponent of TPL will be equal to 2 if and only if the LC model is deterministic; it  
311 will be greater than 2 if the model is supercritical (growing on average) and be less  
312 than 2 if the model is subcritical (declining on average). This property indicates that  
313 parameter  $b = 2$  in our investigation on the Wenchuan earthquake sequence depends  
314 exactly on its specific distribution of aftershocks. In other words, the law of  
315 occurrence of all events or energy release in space and time is deterministic following

316 the main shock on May 12, 2008.

317 Although various empirical confirmations suggest that no specific biological,  
318 physical, technological, or behavioral mechanism can explain all instances of TPL,  
319 there has been some improvement in understanding the distribution and duration time  
320 of aftershocks after the main event. Jiang et al. (2008) studied the Wenchuan  
321 earthquake sequence using Gutenberg–Richter law (1956) and the Omori's law (1894).  
322 Their investigation attained a specific relationship between the magnitude and the  
323 total number of earthquakes for a stable  $b$  value, which indicates that the frequency of  
324 aftershocks decreases roughly with the reciprocal of time after the main shock. One of  
325 the models with physical parameters is the stress triggering mechanism put forward  
326 by Dieterich (1994, 1996). Shen et al. (2013) achieved a good fit between the  
327 observed Wenchuan aftershocks and the analytic solution of the modified Dieterich  
328 model. Their results suggested that the generation of earthquakes is actually related to  
329 the state of fault and can quantitatively describe the temporal evolution of the  
330 aftershock decay. In this sense, the Wenchuan energy sequence satisfies TPL with  
331 slope  $b = 2$ , indicating a stable spatial–temporal dependent energy release caused by  
332 regional stress adjustment and redistribution during the fault revolution after the main  
333 shock.

334 It is possible that there are some interactions among earthquakes with different  
335 magnitudes in an earthquake sequence. This kind of interaction probably derives from  
336 medium stress state of the focus zone where earthquakes happen. The stress field in  
337 the aftershock area is in a rapidly adjusting state when a larger earthquake occurred. It



338 is probable that a light stress adjustment caused by a small earthquake most likely  
339 induces an obvious event in its surroundings in the near future. This process can lead  
340 to aggregation of aftershocks in space and time in extensive areas, causing TPL to  
341 hold for the Wenchuan earthquake energy sequence. However, whether TPL accords  
342 with all earthquake sequences and complies with specific parameters, e.g.,  $b = 2$ ,  
343 needs further investigation.

344 The current study shows that the exponents of TPL for different temporal blocks  
345 for the Wenchuan earthquake sequence are approximately equal to 2 universally. The  
346 estimated intercept could be expressed as a linear equation of the log-transformation  
347 of temporal block A (Figure 6). The goodness of fit of the nonlinear regression is very  
348 high ( $R^2 = 0.9940$  in Figure 6), indicating some interesting underlying mechanism  
349 leading to the occurrence of the aftershocks. The distribution of the energy releases  
350 from aftershocks should be a right-skewed unimodal curve that can be reflected by  
351 magnitude frequency distribution as shown in Figure 1. In fact, Cohen and Xu (2015)  
352 have demonstrated that the correlated sampling variation of the mean and variance of  
353 skewed distributions could account for TPL under random sampling and the estimated  
354 exponent of TPL was proportional to the skewness of the distribution curve. For an  
355 exponential distribution, the variance equals its mean squared. However, in our study,  
356 although the variance of energy releases from aftershocks is similarly proportional to  
357 its mean squared, the coefficient of proportionality (i.e.,  $a$  in Eq. [1]) does rely on the  
358 size of the temporal block. This means that the energy releases from aftershocks  
359 might follow a temporal block-dependent generalized exponential distribution, which

360 should be more complex than the generalized exponential distribution (Gupta and  
361 Kundu, 2007). However, the distribution function for the energy releases from  
362 aftershocks has not been well defined so far. The existing functions for describing a  
363 skewed distribution of energy releases or magnitudes usually belong to pure statistical  
364 models that lack clear physical dynamic mechanism. Our study suggests that further  
365 studies should focus on a temporal block-dependent distribution. However, to provide  
366 a clear mathematical expression for this distribution function is beyond the topic of  
367 this paper. It deserves further investigation.

368 In summary, we attempt to use a new way to investigate a spatio-temporal  
369 distribution property of aftershocks of the Wenchuan earthquake sequence during  
370 2008–2016. In terms of the energy release, the variance of samples in the earthquake  
371 population is shown to have a simple power law relationship as a function of the mean  
372 at different timescales, which gives rise to a TPL, i.e.,  $\sigma^2 = a\mu^b$ , with  $b = 2$ . On the  
373 one hand, the results show that the intercept of the fitted line in linear form  $\log_{10}(\sigma^2)$   
374  $= c + b \times \log_{10}(\mu)$  on a log–log scale, increases as the number of samples and it is  
375 reconfirmed that parameter  $c$  (namely  $\log_{10}(a)$ ) predominantly depends upon the size  
376 of the sampling units (Taylor, 1961). On the other hand, if TPL holds, the estimated  
377 values of parameters  $a$  and  $b$  support the conclusion that the Wenchuan aftershocks  
378 mutually trigger each other and distribute in space and time not randomly but  
379 determinantly and definitely. We fix the exponent of TPL to be 2, and check the  
380 effects of different time divisions on the estimate of the intercept. The result shows  
381 that the intercept acts as a logarithm function of the timescale. It implies that the

382 mean–variance relationship of energy releases from the earthquakes can be predicted  
383 even though we cannot accurately predict the time and location of imminent events.

384

385 **Acknowledgments** The work has been funded from NSFC (National Natural  
386 Science Foundation of China) under grant agreements n 41774084 and National Key  
387 R&D Program of China (Grant no. 2018YFC1503506). P.S. was supported by the  
388 Priority Academic Program Development of Jiangsu Higher Education Institutions.

389

## 390 **References**

391 Ballantyne, IV, F.: The upper limit for the exponent of Taylor's power law is a consequence of  
392 deterministic population growth, *Evolutionary Ecology Research*, 7(8), 1213–1220, 2005.

393 Ballantyne, IV, F., and Kerkhoff, A. J.: The observed range for temporal mean–variance scaling  
394 exponents can be explained by reproductive correlation, *Oikos*, 116(1), 174–180, 2007.

395 Burchfiel, B. C., Royden, L. H., van der Hilst, R. D., Hager, B. H., Chen, Z., King, R. W., Li, C.,  
396 Lu, J., Yao, H., and Kirby, E.: A geological and geophysical context for the Wenchuan earthquake of  
397 12 May 2008, Sichuan, People's Republic of China, *GSA Today*, 18(7), 4–11, 2008,  
398 doi:10.1130/GSATG18A.1.

399 Chen, Y., Xu, L., Zhang, Y., Du, H., Feng, W., Liu, C., and Li, C.: Report on source  
400 characteristics of the larger Wenchuan earthquake source on May 12, 2008, 2008,  
401 <http://www.csi.ac.cn/Sichuan/chenyuntai.pdf> (in Chinese).

402 Cohen, J. E.: Taylor's power law of fluctuation scaling and the growth–rate theorem, *Theoretical*  
403 *Population Biology*, 88, 94–100, 2013.

404 Cohen, J. E., and Xu, M.: Random sampling of skewed distributions implies Taylor's power law of  
405 fluctuation scaling, *Proc Natl Acad Sci USA*, 112(25), 7749–7754, 2015,  
406 doi.org/10.1073/pnas.1503824112.

407 Console, R., Jackson, D. D., and Kagan, Y. Y.: Using the ETAS model for catalog declustering and  
408 seismic background assessment, *Pure & Applied Geophysics*, 167(6–7), 819–830, 2010,  
409 doi.org/10.1007/s00024–010–0065–5.

410 Dieterich, J. H.: A constitutive law for rate of earthquake production and its application to  
411 earthquake clustering, *J. Geophys. Res.*, 99(B2), 2601–2618, 1994.

412 Dieterich, J. H., and Kilgore, B.: Implications of fault constitutive properties for earthquake

413 prediction, *Proceedings of the National Academy of Sciences*, 93(9), 3787–3794, 1996.

414 Eisler, Z., Bartos, I., and Kertész, J.: Fluctuation scaling in complex systems: Taylor's law and  
415 beyond, *Advances in Physics*, 57(1), 89–142, 2008, doi.org/10.1080/00018730801893043.

416 Gupta, R.D., and Kundu, D.: Generalized exponential distribution: Existing results and some  
417 recent developments, *Journal of Statistical Planning and Inference*, 137, 3537–3547, 2007,  
418 doi:10.1016/j.jspi.2007.03.030.

419 Gutenberg, B., and Richter, C. F.: Magnitude and energy of earthquakes, *Annali di Geofisica*, 9,  
420 1–15, 1956.

421 Harris, R. A.: Introduction to special section: stress triggers, stress shadows, and implications for  
422 seismic hazard, *J. Geophys. Res.: Solid Earth*, 103(B10), 24347–24358, 1998,  
423 doi.org/10.1029/98JB01576.

424 Horne, J. K., and Schneider, D. C.: Spatial variance in ecology, *Oikos*, 74, 18–26, 1995.

425 Jiang, H. K., Li, M. X., Wu, Q., and Song, J.: Features of the May 12 *M* 8.0 Wenchuan earthquake  
426 sequence and discussion on relevant problems, *Seismology and geology*, 30(3), 746–758, 2008 (In  
427 Chinese with English abstract).

428 Kendal, W. S.: A frequency distribution for the number of hematogenous organ metastases,  
429 *Journal of Theoretical Biology*, 217(2), 203–218, 2002.

430 Kilpatrick, A. M., and Ives, A. R.: Species interactions can explain Taylor's power law for  
431 ecological time series, *Nature*, 422(6927), 65–68, 2003.

432 Kumazawa, T., and Ogata, Y.: Quantitative description of induced seismic activity before and  
433 after 2011 Tohoku Oki–earthquake by nonstationary ETAS models, *J. Geophys. Res.: Solid Earth*,  
434 118(12), 6165–6182, 2013, doi:10.1002/2013JB010259.

435 Lin, S., Shao, L., Hui, C., Sandhu, H. S., Fan, T., Zhang, L., Li, F., Ding, Y., and Shi, P.: The  
436 effect of temperature on the developmental rates of seedling emergence and leaf-unfolding in two  
437 dwarf bamboo species, *Trees Struct Funct*, 32, 751–763, 2018.

438 Maurer, B. A., and Taper, M. L.: Connecting geographical distributions with population processes,  
439 *Ecology Letters*, 5(2), 223–231, 2010.

440 McCaffrey, R.: Earthquakes and crustal deformation, In Harsh K. Gupta (ed.), *Encyclopedia of*  
441 *Solid Earth Geophysics*, 218–226, 2011, doi: 10.1007/978-90-481-8702-7.

442 Ogata, Y.: Statistical models for earthquake occurrences and residual analysis for point processes,  
443 *J. Am. Stat. Assoc*, 83(407), 9–27, 1988.

444 Ogata, Y.: Statistical model for standard seismicity and detection of anomalies by residual  
445 analysis, *Tectonophysics*, 169(1), 159–174, 1989.

446 Ogata, Y.: Seismicity analysis through point–process modeling: A review, *Pure Appl. Geophys.*,  
447 155(2–4), 471–507, 1999.

448 Omori, F.: On the aftershocks of earthquakes. *Journal of the College of Science, Imperial*  
449 *University of Tokyo*, 7, 111–200, 1894.

450 Robinson, R., and Zhou, S.: Stress interactions within the Tangshan, China, earthquake sequence  
451 of 1976, *Bull Seism Soc Amer*, 85(6), 2501–2505, 2005.

452 Shi, P.J., Sandhu, H. S., and Reddy, G.V.P.: Dispersal distance determines the exponent of the  
453 spatial Taylor's power law, *Ecol Model*, 335, 48–53, 2016.

454 Shi, P.J., Ratkowsky, D. A., Wang, N. T., Li, Y., Reddy, G. V. P., Zhao, L., and Li, B. L.:  
455 Comparison of five methods for parameter estimation under Taylor's power law, *Ecol Compl.*, 32,  
456 121–130, 2017.

457 Stein, R. S.: The role of stress transfer in earthquake occurrence, *Nature*, 402, 605–609, 1999.

458 Taylor, L.R.: Aggregation, variance and the mean, *Nature*, 189, 732–735, 1961,  
459 doi:10.1038/189732a0.

460 Taylor, L. R.: Assessing and interpreting the spatial distributions of insect populations,  
461 *Entomology*, 29(1), 321–357, 1984.

462 Utsu, T.: Aftershocks and earthquake statistics (1): some parameters which characterize an  
463 aftershock sequence and their interrelations, *Journal of the Faculty of Science Hokkaido University*,  
464 3(3), 129–195, 1969.

465 Utsu, T., Ogata, Y., Ritsuko, S., and Matsu'ura: The centenary of the Omori formula for a decay  
466 law of aftershock activity, *Earth Planets & Space*, 43(1), 1–33, 2009.

467 Vere-Jones, D., Ben-Zion, Y., and Zuniga, R.: Statistical seismology, *Pure Appl Geophys.*, 162,  
468 1023–1026, 2005.

469 Xu, G. M., and Zhou, H. L.: *Principle of Earthquake*, Science Publication House, p325–352, 1982.